Assessing Regional Climate Model Predictions

Bruno Sansó

Department of Applied Mathematics and Statistics
University of California Santa Cruz
http://www.ams.ucsc.edu/∼bruno

Climate Models use the equations of motion to simulate changes in the global phenomena of the atmosphere. General Climate Models (GCM) describe large scale global motions and have the goal of describing long term changes in the atmosphere.

Climate Models use the equations of motion to simulate changes in the global phenomena of the atmosphere. General Climate Models (GCM) describe large scale global motions and have the goal of describing long term changes in the atmosphere.

Regional Climate Models (RCM) produce a "dynamic downscaling" of the output of GCMs. They simulate relatively short-term atmospheric and land-surface processes and the interactions between the two, at a spatial resolution of about 50 km.

There are a number of sources of uncertainties related to climate model assessment:

Climate Model Uncertainties

There are a number of sources of uncertainties related to climate model assessment:

- Uncertainty regarding the parameterization of subgrid-scale processes.

Climate Model Uncertainties

There are a number of sources of uncertainties related to climate model assessment:

- Uncertainty regarding the parameterization of subgrid-scale processes.
- Uncertainty regarding the initial conditions.

Climate Model Uncertainties

There are a number of sources of uncertainties related to climate model assessment:

- Uncertainty regarding the parameterization of subgrid-scale processes.
- Uncertainty regarding the initial conditions.
- Uncertainty regarding the structure of the climate model simulator.

There are a number of sources of uncertainties related to climate model assessment:

- Uncertainty regarding the parameterization of subgrid-scale processes.
- Uncertainty regarding the initial conditions.
- Uncertainty regarding the structure of the climate model simulator.
- Uncertainty regarding the historical records.

There are a number of sources of uncertainties related to climate model assessment:

- Uncertainty regarding the parameterization of subgrid-scale processes.
- Uncertainty regarding the initial conditions.
- Uncertainty regarding the structure of the climate model simulator.
- Uncertainty regarding the historical records.

In this talk we focus on the multi-model uncertainty.

Denote as $F(\boldsymbol{\theta})$ the output from a computer model depending on parameter $\boldsymbol{\theta}$. let Y denote a set of observations corresponding to $F(\boldsymbol{\theta})$.

Denote as $F(\boldsymbol{\theta})$ the output from a computer model depending on parameter $\boldsymbol{\theta}$. let Y denote a set of observations corresponding to $F(\boldsymbol{\theta})$.

The traditional setting for assessment and calibration of a computer model assumes that both, model and observations provide information about a true, unobserved quantity, say ξ. Then

$$Y = \xi + \varepsilon, \quad \text{and} \quad F(\boldsymbol{\theta}) = \xi + \delta$$

where ε is observational error and δ is model discrepancy.

- Estimation of δ provides an assessment of the model

- Estimation of δ provides an assessment of the model
- Estimation of $\boldsymbol{\theta}$ provides a calibration of the model.

- Estimation of δ provides an assessment of the model
- Estimation of $\boldsymbol{\theta}$ provides a calibration of the model.
- Estimation of ξ provides information about the property of interest, using both simulations and observations.

Is it fair to compare climate model simulations for, say, a given year to the corresponding observational records?

Is it fair to compare climate model simulations for, say, a given year to the corresponding observational records?

A simulation indexed by a given year is not meant to reproduce that year's observations. It is just a sample from the climate that is typical of that year, as estimated by the climate model.

Is it fair to compare climate model simulations for, say, a given year to the corresponding observational records?

A simulation indexed by a given year is not meant to reproduce that year's observations. It is just a sample from the climate that is typical of that year, as estimated by the climate model.

To tackle this issue we can:

- Average over large areas and time spans.
- Consider large scale summaries of the spatial and temporal fields, i.e. trends, cycles, patterns, indexes.
- Use Space-time models for smoothing.

NARCCAP DOMAIN

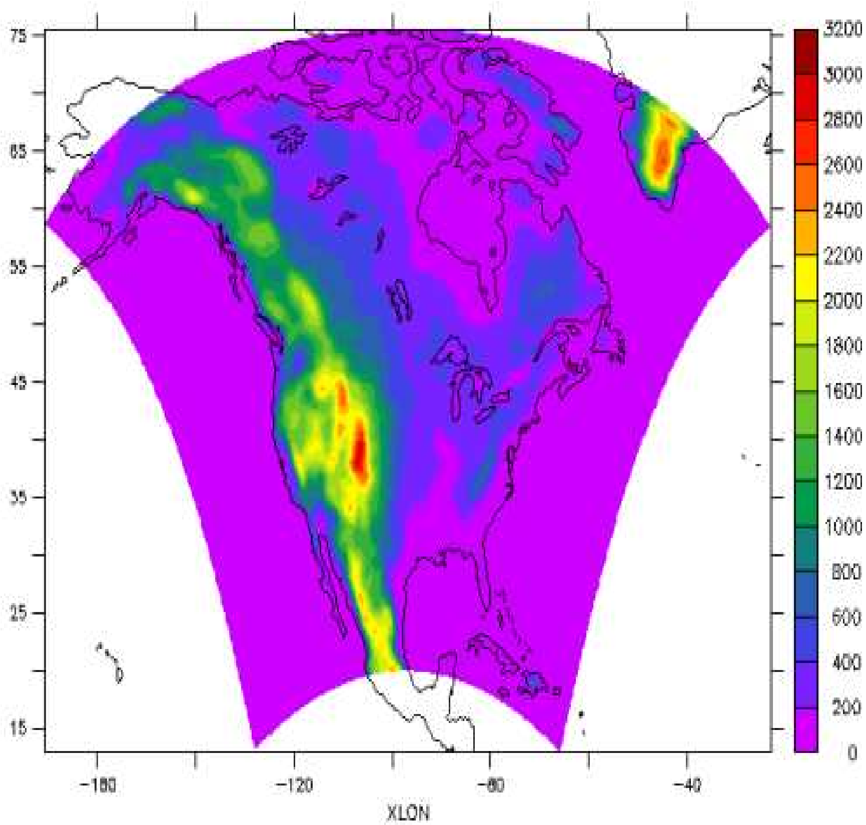

- NARCCAP is a program to produce high resolution climate change simulations over the US, Canada and Mexico.

NARCCAP Domain

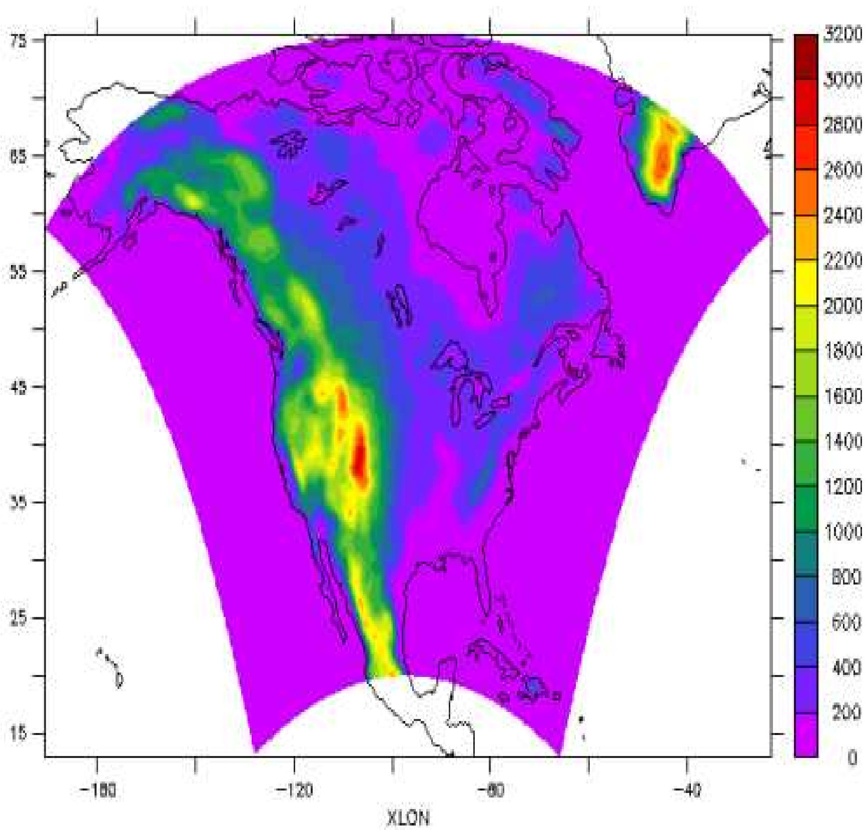

- NARCCAP is a program to produce high resolution climate change simulations over the US, Canada and Mexico.
- The goal is to assess climate variability at a regional level.

NARCCAP Domain

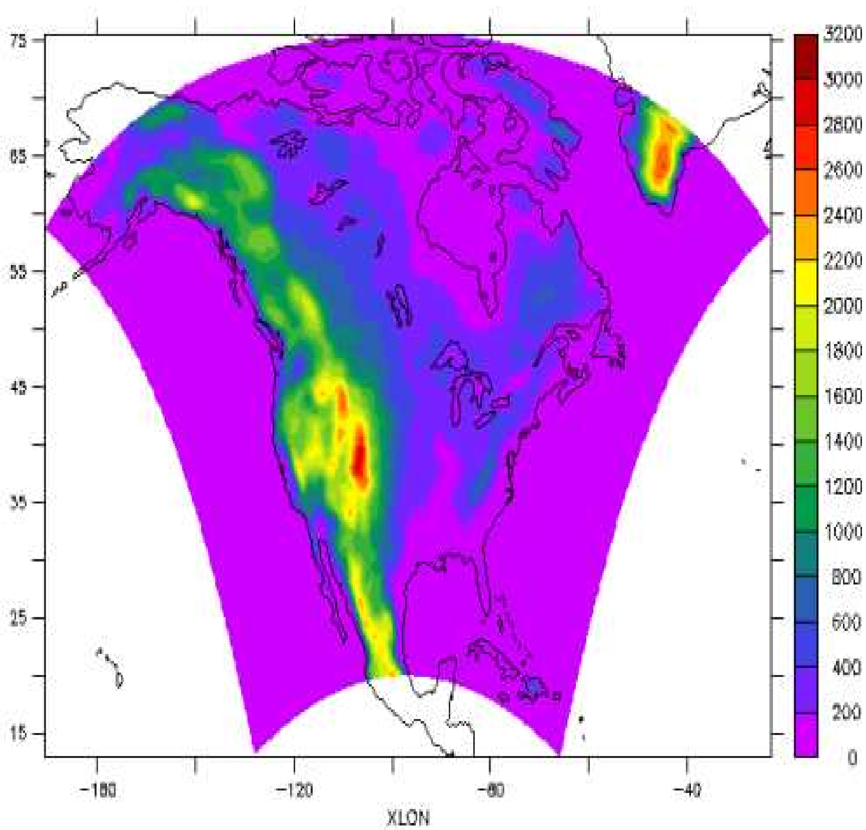

- NARCCAP is a program to produce high resolution climate change simulations over the US, Canada and Mexico.
- The goal is to assess climate variability at a regional level.
- All RCMs use the same 50 km resolution and the same future emission scenario (A2)

NARCCAP Combinations

- NARCCAP considers six different RCMs, four different AOGCM, NCEP reanalysis and two time slices.

NARCCAP Combinations

	AOGCMs			
RCMs	GFDL	HADCM3	CGCM3	CCSM
RegCM3	X		X	
ECPC	X	X		
PRECIS	X	X		
CRCM			X	X
WRF			X	X
MM5		X		X

- NARCCAP considers six different RCMs, four different AOGCM, NCEP reanalysis and two time slices.
- Not every combination of the RCMs and the AOGCM are considered, so the experiment resulted in a fractional factorial design.

NARCCAP Combinations

	AOGCMs			
RCMs	GFDL	HADCM3	CGCM3	CCSM
RegCM3	X		X	
ECPC	X	X		
PRECIS	X	X		
CRCM			X	X
WRF			X	X
MM5		X		X

- NARCCAP considers six different RCMs, four different AOGCM, NCEP reanalysis and two time slices.
- Not every combination of the RCMs and the AOGCM are considered, so the experiment resulted in a fractional factorial design.
- All models consider present day conditions from 1971 to 2000 and future simulations 2041 to 2070.

NARCCAP Combinations

	AOGCMs			
RCMs	GFDL	HADCM3	CGCM3	CCSM
RegCM3	X		X	
ECPC	X	X		
PRECIS	X	X		
CRCM			X	X
WRF			X	X
MM5		X		X

The Domain of our Analysis

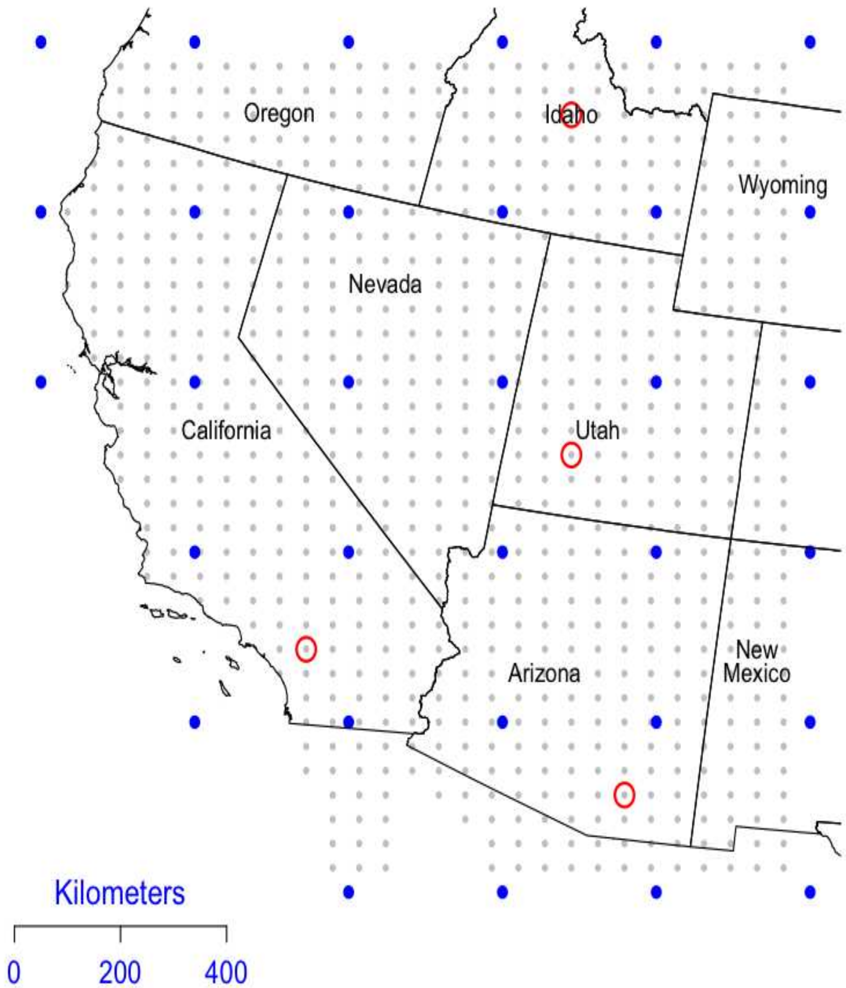

- We focus on the Southwest corner of the US. The gray dots correspond to the 50 km resolution of the RCMs.

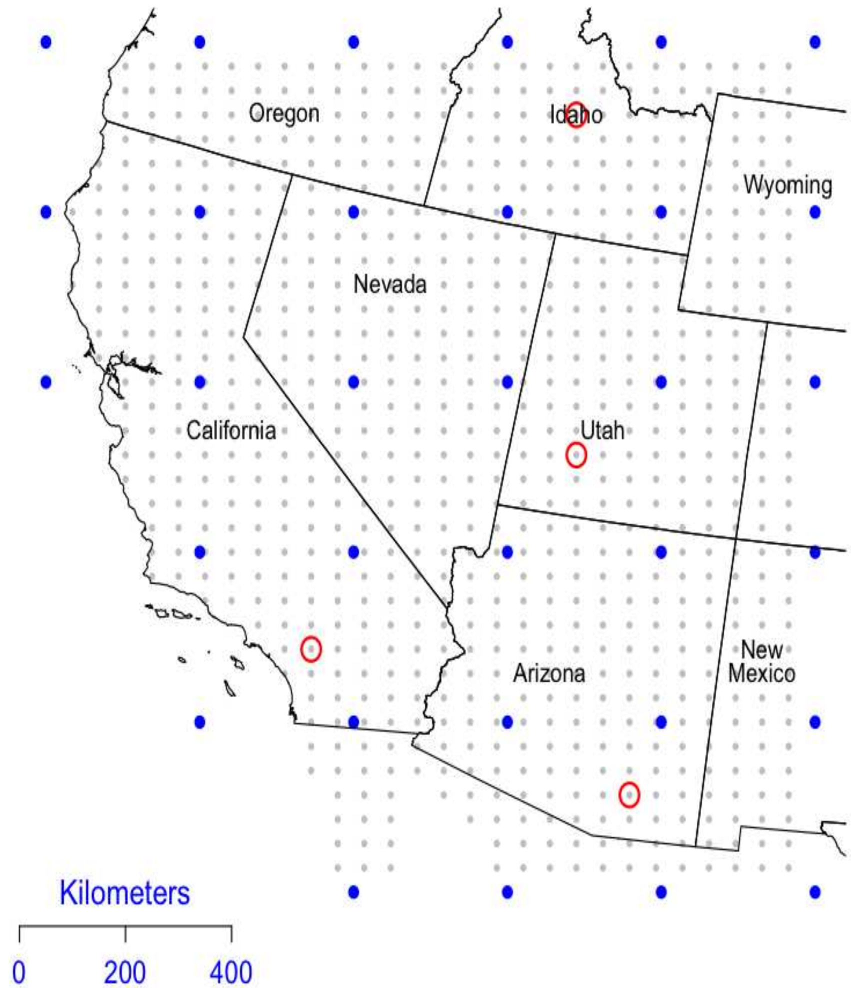

- We focus on the Southwest corner of the US. The gray dots correspond to the 50 km resolution of the RCMs.
- We consider the simulations obtained using RegCM3 under NCEP, GFDL and CGCM3 forcings.

The Domain of our Analysis

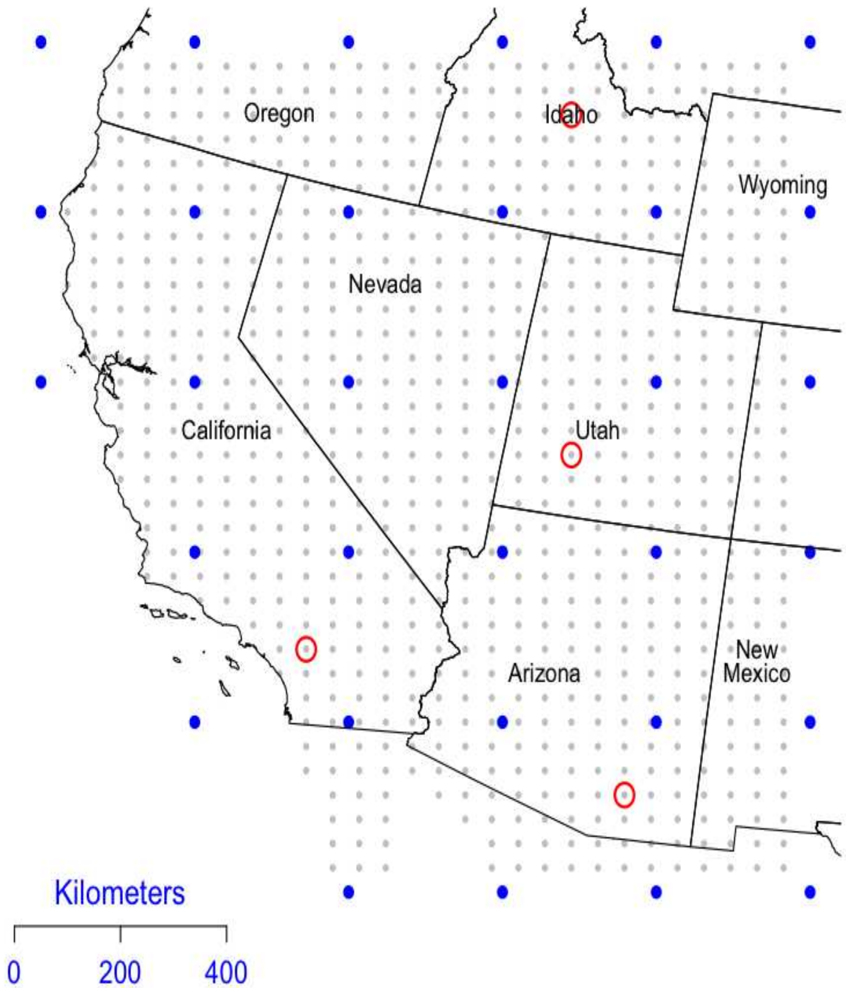

- We focus on the Southwest corner of the US. The gray dots correspond to the 50 km resolution of the RCMs.
- We consider the simulations obtained using RegCM3 under NCEP, GFDL and CGCM3 forcings.
- We study the variability of yearly mean summer temperature at each of the 802 locations.

- We use NARCCAP simulations of mean summer temperature.

These correspond to three hour periods for 802 grid cells.

Data Description and Processing

- We use NARCCAP simulations of mean summer temperature. These correspond to three hour periods for 802 grid cells.

- We used weather station temperature measurements collected by the NCDC. They are available at three hour intervals for a variable number of locations, depending on the year, ranging from a min. of 56, to a max. of 262, with a median of 198.

Data Description and Processing

- We use NARCCAP simulations of mean summer temperature. These correspond to three hour periods for 802 grid cells.

- We used weather station temperature measurements collected by the NCDC. They are available at three hour intervals for a variable number of locations, depending on the year, ranging from a min. of 56, to a max. of 262, with a median of 198.

- To obtain interpolated fields we processed 3 hour data by detrending using location and elevation. We then estimated exponential variogram parameters with nugget.

Data Description and Processing

- We use NARCCAP simulations of mean summer temperature. These correspond to three hour periods for 802 grid cells.

- We used weather station temperature measurements collected by the NCDC. They are available at three hour intervals for a variable number of locations, depending on the year, ranging from a min. of 56, to a max. of 262, with a median of 198.

- To obtain interpolated fields we processed 3 hour data by detrending using location and elevation. We then estimated exponential variogram parameters with nugget.

- We did a simple kriging of the residuals and then averaged of all the 3 hourly values.

- Validate the RCM simulations with respect to the observational records.

- Validate the RCM simulations with respect to the observational records.
- Compare the RCM simulations temporally and spatially. A one way spatio-temporal ANOVA.

Goals

- Validate the RCM simulations with respect to the observational records.
- Compare the RCM simulations temporally and spatially. A one way spatio-temporal ANOVA.
- Explore trends of spatial and temporal variability that are common for the four sources of information.

- Validate the RCM simulations with respect to the observational records.
- Compare the RCM simulations temporally and spatially. A one way spatio-temporal ANOVA.
- Explore trends of spatial and temporal variability that are common for the four sources of information.
- Merge the four data sources to obtain blended reconstructions and forecasts, including probabilistic measures of uncertainty.

Averages Over Space

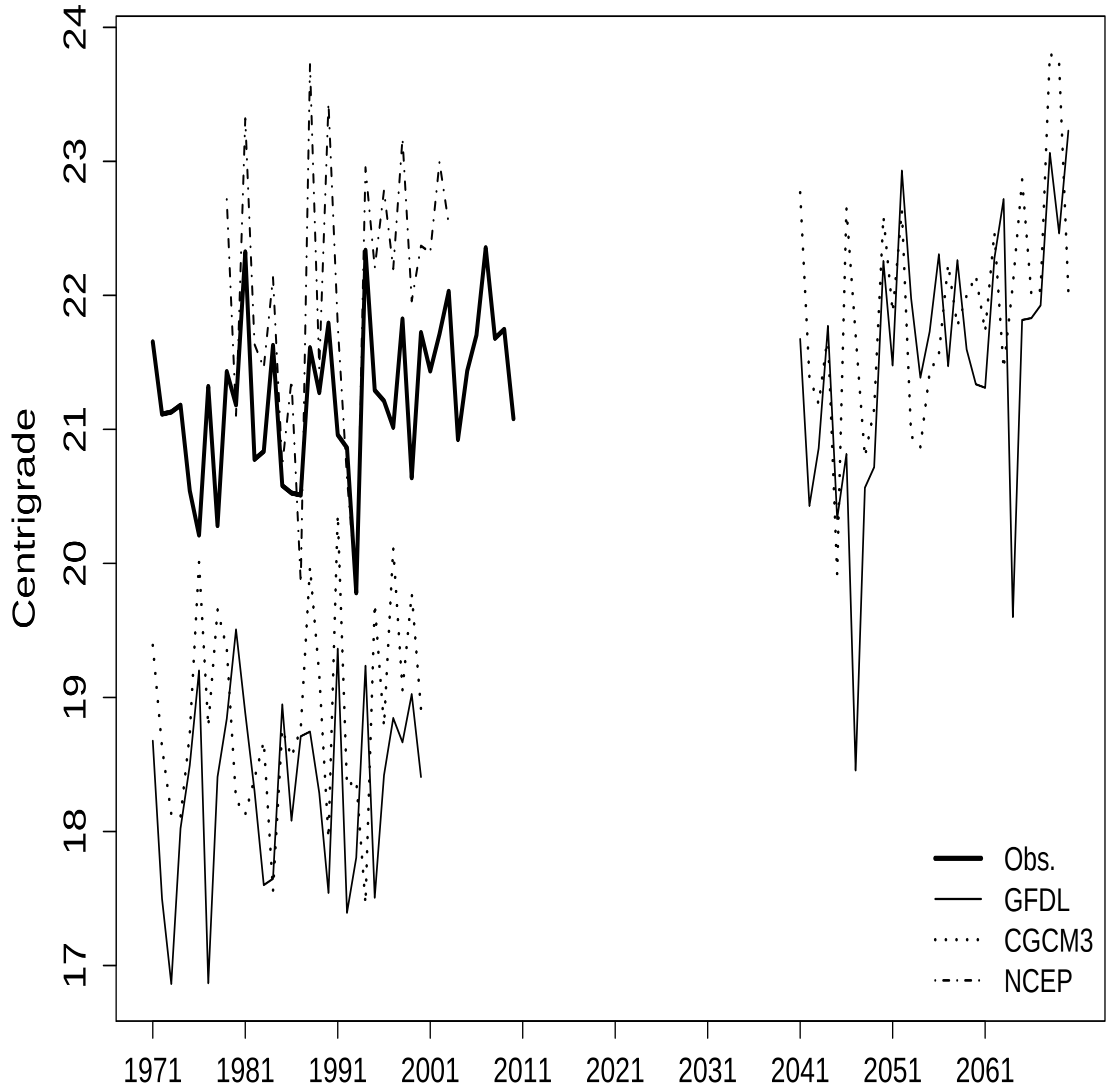

Note the gap in the first part of the 21st Cent., and the discrepancy between obs. and simul. during the 20th Cent. for CGCM3 and GFDL.

Observations

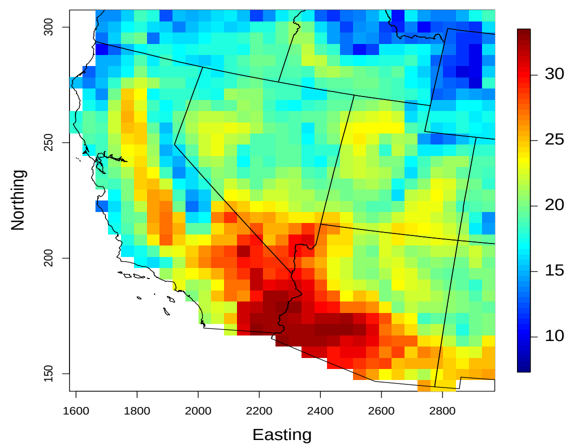

NCEP

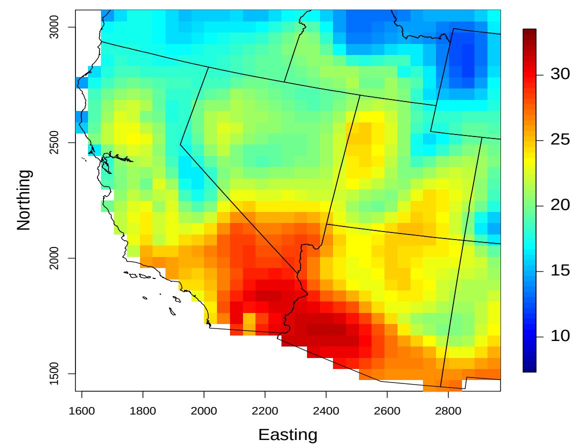

GFDL

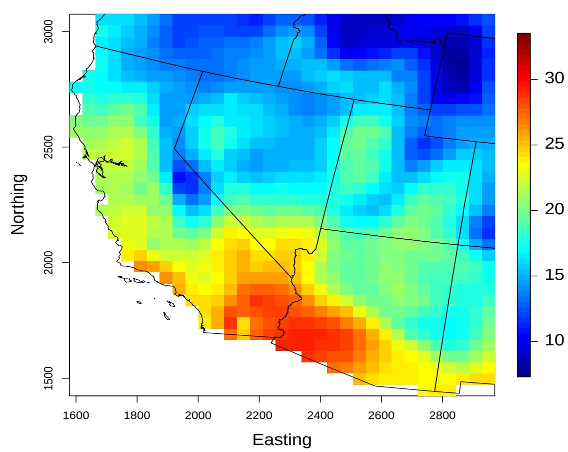

CGCM3

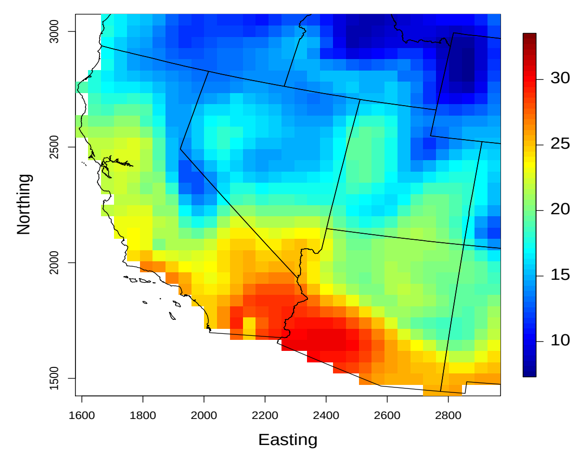

We use a small number of components to explain the temporal and spatial variability. This provides computational advantages as well as estimation of the modes of main spatial variability.

We use a small number of components to explain the temporal and spatial variability. This provides computational advantages as well as estimation of the modes of main spatial variability.

All four data sources correspond to a common space-time process. RCMs deviations from that process are time and space varying.

$$
\begin{aligned}
y_t(\boldsymbol{s}) &= \boldsymbol{x}_t^T(\boldsymbol{s})\eta + \xi(t-t_0) + \omega_t(\boldsymbol{s}) + \qquad\qquad\qquad + \epsilon_t(\boldsymbol{s}) \\
y_{jt}^{CM}(\boldsymbol{s}) &= \underbrace{\boldsymbol{x}_t^T(s)\eta}_{\text{covariates}} + \underbrace{\xi(t-t_0)}_{\text{trend}} + \underbrace{\omega_t(\boldsymbol{s})}_{\text{baseline}} + \underbrace{d_{jt}(\boldsymbol{s})}_{\text{discrepancy}} + \epsilon_{jt}(\boldsymbol{s})
\end{aligned}
$$

$\epsilon_t(\boldsymbol{s})$ and $\epsilon_{jt}(\boldsymbol{s})$ are observational errors.

The dimensionality of $\omega_t(\boldsymbol{s})$ is reduced with a predictive Gaussian process approach:

$$\omega_t(\boldsymbol{s}) = \sum_{m=1}^{M} B_m(\boldsymbol{s})\gamma_{m,t} + \tilde{\varepsilon}_t(\boldsymbol{s}) = \boldsymbol{B}(\boldsymbol{s})^T \boldsymbol{\gamma}_t + \tilde{\varepsilon}_t(\boldsymbol{s})$$

The dimensionality of $\omega_t(\boldsymbol{s})$ is reduced with a predictive Gaussian process approach:

$$\omega_t(\boldsymbol{s}) = \sum_{m=1}^{M} B_m(\boldsymbol{s})\gamma_{m,t} + \tilde{\varepsilon}_t(\boldsymbol{s}) = \boldsymbol{B}(\boldsymbol{s})^T \boldsymbol{\gamma}_t + \tilde{\varepsilon}_t(\boldsymbol{s})$$

$B_m(\boldsymbol{s}) = [\boldsymbol{v}(\boldsymbol{s})^T \boldsymbol{H}^{-1}]_m,\ \boldsymbol{\gamma}_t \sim N(\varphi\boldsymbol{\gamma}_{t-1}, \boldsymbol{H})$ and $\tilde{\varepsilon}_t(\boldsymbol{s}) \sim N(0, \tau^2 - \boldsymbol{v}(\boldsymbol{s})^T \boldsymbol{H}^{-1} \boldsymbol{v}(\boldsymbol{s}))$.

The dimensionality of $\omega_t(\boldsymbol{s})$ is reduced with a predictive Gaussian process approach:

$$\omega_t(\boldsymbol{s}) = \sum_{m=1}^{M} B_m(\boldsymbol{s})\gamma_{m,t} + \tilde{\varepsilon}_t(\boldsymbol{s}) = \boldsymbol{B}(\boldsymbol{s})^T \boldsymbol{\gamma}_t + \tilde{\varepsilon}_t(\boldsymbol{s})$$

$B_m(\boldsymbol{s}) = [\boldsymbol{v}(\boldsymbol{s})^T \boldsymbol{H}^{-1}]_m$, $\boldsymbol{\gamma}_t \sim N(\varphi \boldsymbol{\gamma}_{t-1}, \boldsymbol{H})$ and $\tilde{\varepsilon}_t(\boldsymbol{s}) \sim N(0, \tau^2 - \boldsymbol{v}(\boldsymbol{s})^T \boldsymbol{H}^{-1} \boldsymbol{v}(\boldsymbol{s}))$.

$\boldsymbol{v}(\boldsymbol{s}) = \tau^2(\rho(\boldsymbol{s}, \boldsymbol{s}_1^*; \boldsymbol{\phi}), \ldots, \rho(\boldsymbol{s}, \boldsymbol{s}_M^*; \boldsymbol{\phi}))$ and $H_{lk} = \tau^2 \rho(\boldsymbol{s}_l^*, \boldsymbol{s}_k^*; \boldsymbol{\phi})$.

$\boldsymbol{\gamma}_t$ is a Gaussian process on the set of points $\{\boldsymbol{s}_1^*, \ldots, \boldsymbol{s}_M^*\}$. Its correlation function ρ is the Matèrn with parameters $\boldsymbol{\phi} = (\phi_1, \phi_2)$.

$\boldsymbol{\gamma}_t$ is a Gaussian process on the set of points $\{\boldsymbol{s}_1^*, \ldots, \boldsymbol{s}_M^*\}$. Its correlation function ρ is the Matèrn with parameters $\boldsymbol{\phi} = (\phi_1, \phi_2)$.

$\omega_t(\boldsymbol{s})$ is the predictive expectation of $\gamma_t(\boldsymbol{s}^*)$ at location $\boldsymbol{s}$.

$\boldsymbol{\gamma}_t$ is a Gaussian process on the set of points $\{\boldsymbol{s}_1^*, \ldots, \boldsymbol{s}_M^*\}$. Its correlation function ρ is the Matèrn with parameters $\boldsymbol{\phi} = (\phi_1, \phi_2)$.

$\omega_t(\boldsymbol{s})$ is the predictive expectation of $\gamma_t(\boldsymbol{s}^*)$ at location $\boldsymbol{s}$.

In our application $M = 32$ and the sites $\boldsymbol{s}_m^*$ are located on a regular grid with a resolution of 290 km.

Consider the spectral decomposition $\boldsymbol{H} = \boldsymbol{P}\boldsymbol{\Lambda}\boldsymbol{P}^T$, $\boldsymbol{P}$ orthogonal and $\boldsymbol{\Lambda}$ diagonal. Let $\boldsymbol{\gamma}_t = \boldsymbol{P}\boldsymbol{\alpha}_t$, $\forall t$, then

$$\omega_t(\boldsymbol{s}) = \boldsymbol{B}(\boldsymbol{s})^T \boldsymbol{P}\boldsymbol{\alpha}_t = \boldsymbol{\psi}(\boldsymbol{s})^T \boldsymbol{\alpha}_t \text{ and } \boldsymbol{\alpha}_t \sim N(\varphi \boldsymbol{\alpha}_{t-1}, \boldsymbol{\Lambda}).$$

Consider the spectral decomposition $\boldsymbol{H} = \boldsymbol{P}\boldsymbol{\Lambda}\boldsymbol{P}^T$, $\boldsymbol{P}$ orthogonal and $\boldsymbol{\Lambda}$ diagonal. Let $\boldsymbol{\gamma}_t = \boldsymbol{P}\boldsymbol{\alpha}_t$, $\forall t$, then

$$\omega_t(\boldsymbol{s}) = \boldsymbol{B}(\boldsymbol{s})^T \boldsymbol{P}\boldsymbol{\alpha}_t = \boldsymbol{\psi}(\boldsymbol{s})^T \boldsymbol{\alpha}_t \text{ and } \boldsymbol{\alpha}_t \sim N(\varphi \boldsymbol{\alpha}_{t-1}, \boldsymbol{\Lambda}).$$

A similar representation for d_{jt} yields

$$\omega_t(\boldsymbol{s}) + d_{jt}(\boldsymbol{s}) = \boldsymbol{B}(\boldsymbol{s})^T(\boldsymbol{\gamma}_t + \boldsymbol{\gamma}_{jt}) = \boldsymbol{\psi}(\boldsymbol{s})^T(\boldsymbol{\alpha}_t + \boldsymbol{\alpha}_{jt}),$$

and

$$\boldsymbol{\alpha}_{jt} \sim N(\varphi_j \boldsymbol{\alpha}_{j,t-1}, \boldsymbol{\Lambda}_j).$$

Consider the spectral decomposition $\boldsymbol{H} = \boldsymbol{P}\boldsymbol{\Lambda}\boldsymbol{P}^T$, $\boldsymbol{P}$ orthogonal and $\boldsymbol{\Lambda}$ diagonal. Let $\boldsymbol{\gamma}_t = \boldsymbol{P}\boldsymbol{\alpha}_t$, $\forall t$, then

$$\omega_t(\boldsymbol{s}) = \boldsymbol{B}(\boldsymbol{s})^T \boldsymbol{P}\boldsymbol{\alpha}_t = \boldsymbol{\psi}(\boldsymbol{s})^T \boldsymbol{\alpha}_t \text{ and } \boldsymbol{\alpha}_t \sim N(\varphi \boldsymbol{\alpha}_{t-1}, \boldsymbol{\Lambda}).$$

A similar representation for d_{jt} yields

$$\omega_t(\boldsymbol{s}) + d_{jt}(\boldsymbol{s}) = \boldsymbol{B}(\boldsymbol{s})^T(\boldsymbol{\gamma}_t + \boldsymbol{\gamma}_{jt}) = \boldsymbol{\psi}(\boldsymbol{s})^T(\boldsymbol{\alpha}_t + \boldsymbol{\alpha}_{jt}),$$

and

$$\boldsymbol{\alpha}_{jt} \sim N(\varphi_j \boldsymbol{\alpha}_{j,t-1}, \boldsymbol{\Lambda}_j).$$

The fields $\psi_m(\boldsymbol{s})$ are not orthogonal, but the corresponding coefficients are independent with decreasing variance.

$\Psi_{(1)}$

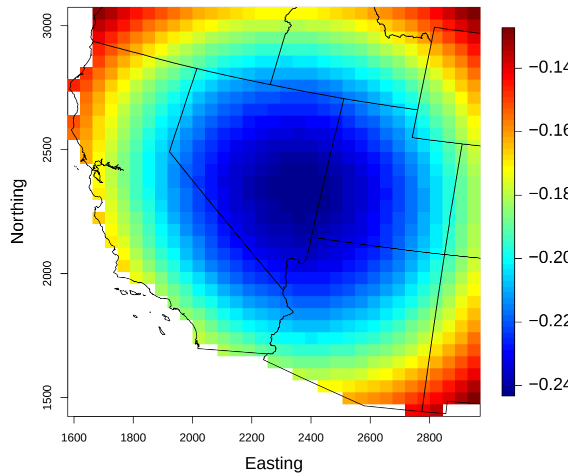

$\Psi_{(2)}$

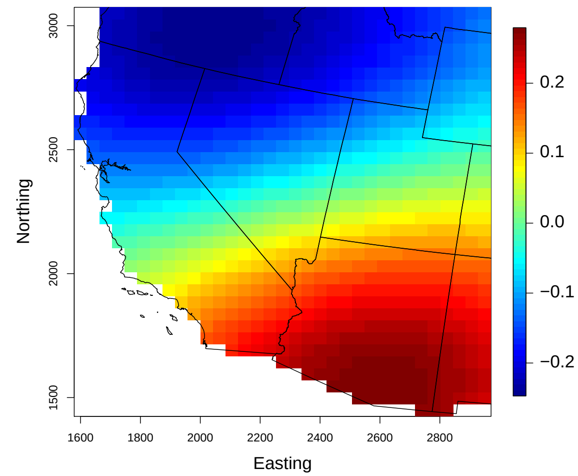

$\Psi_{(3)}$

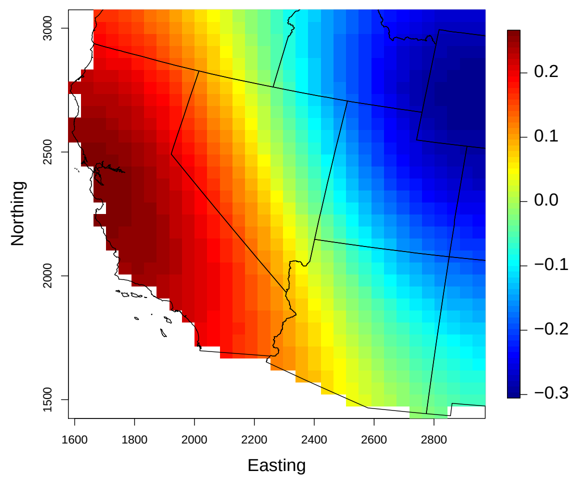

$\Psi_{(4)}$

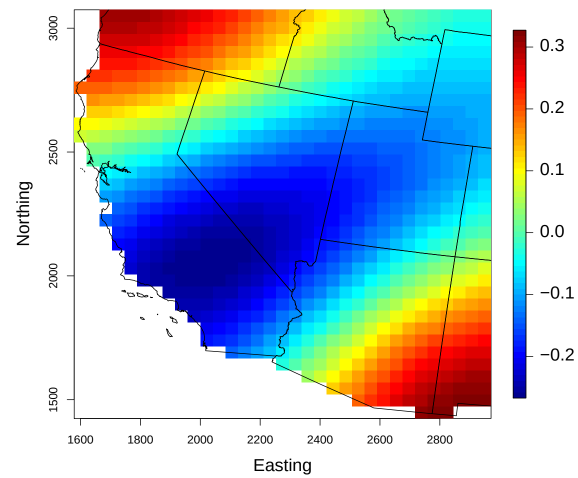

First Factor Coefficients

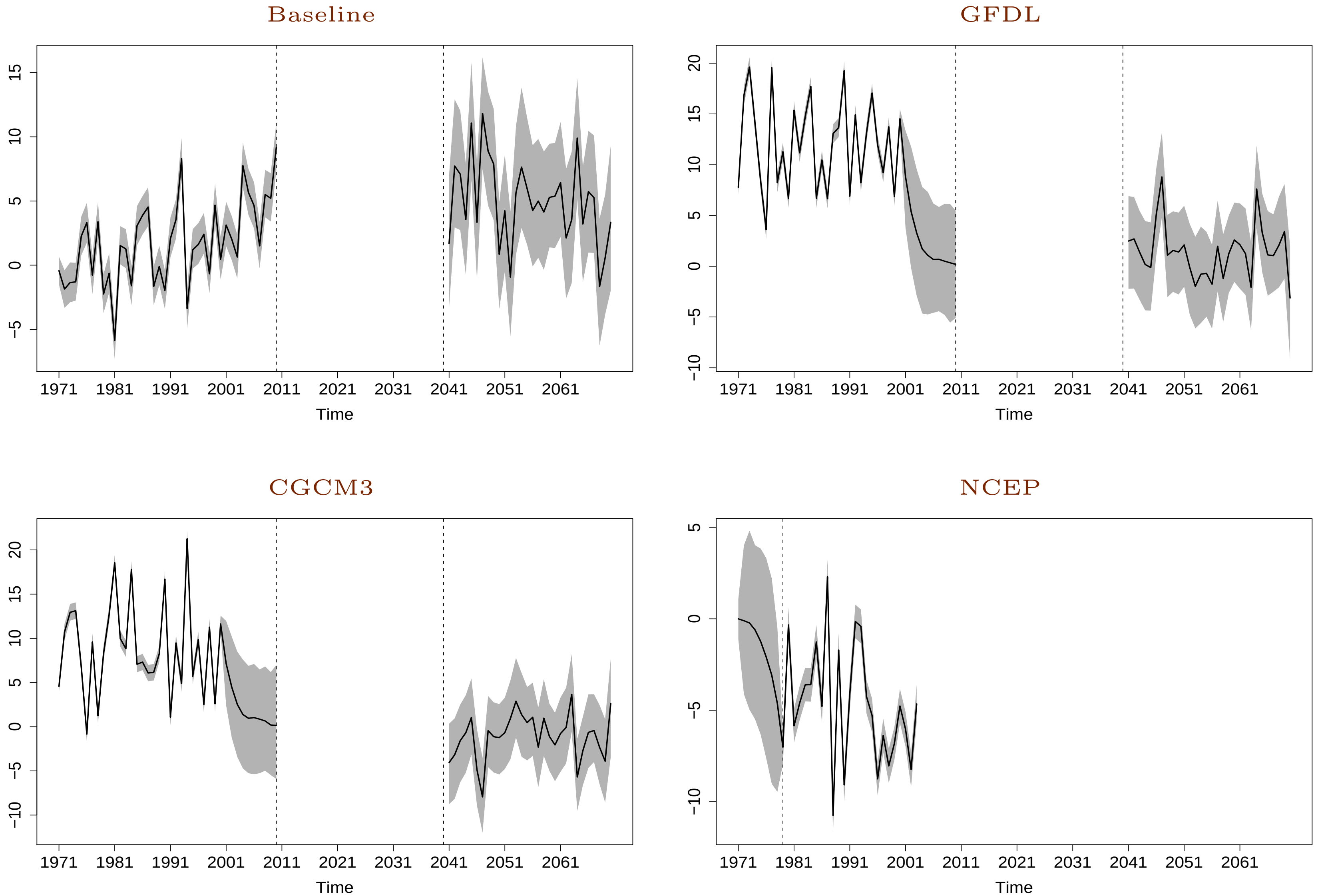

Second Factor Coefficients

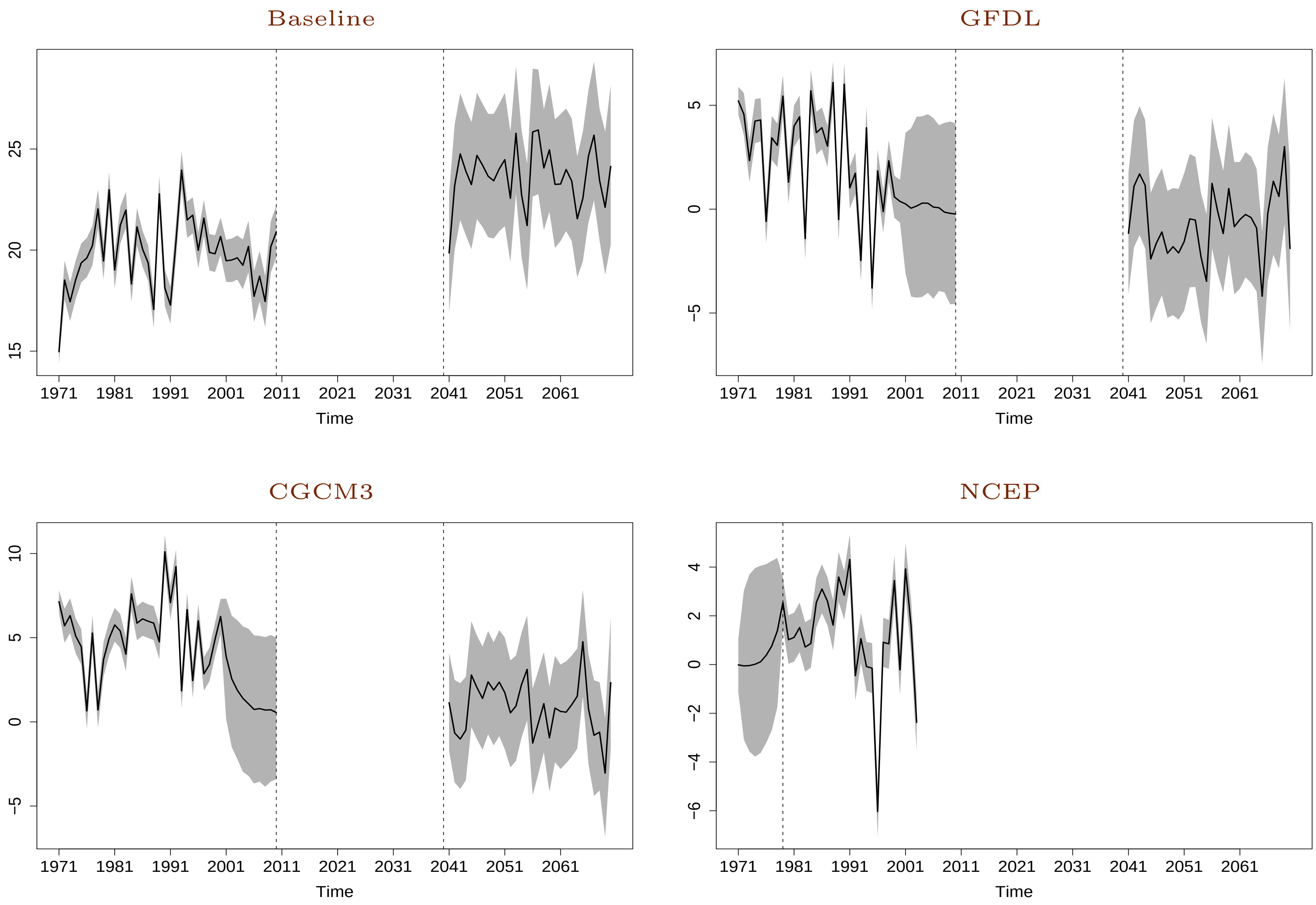

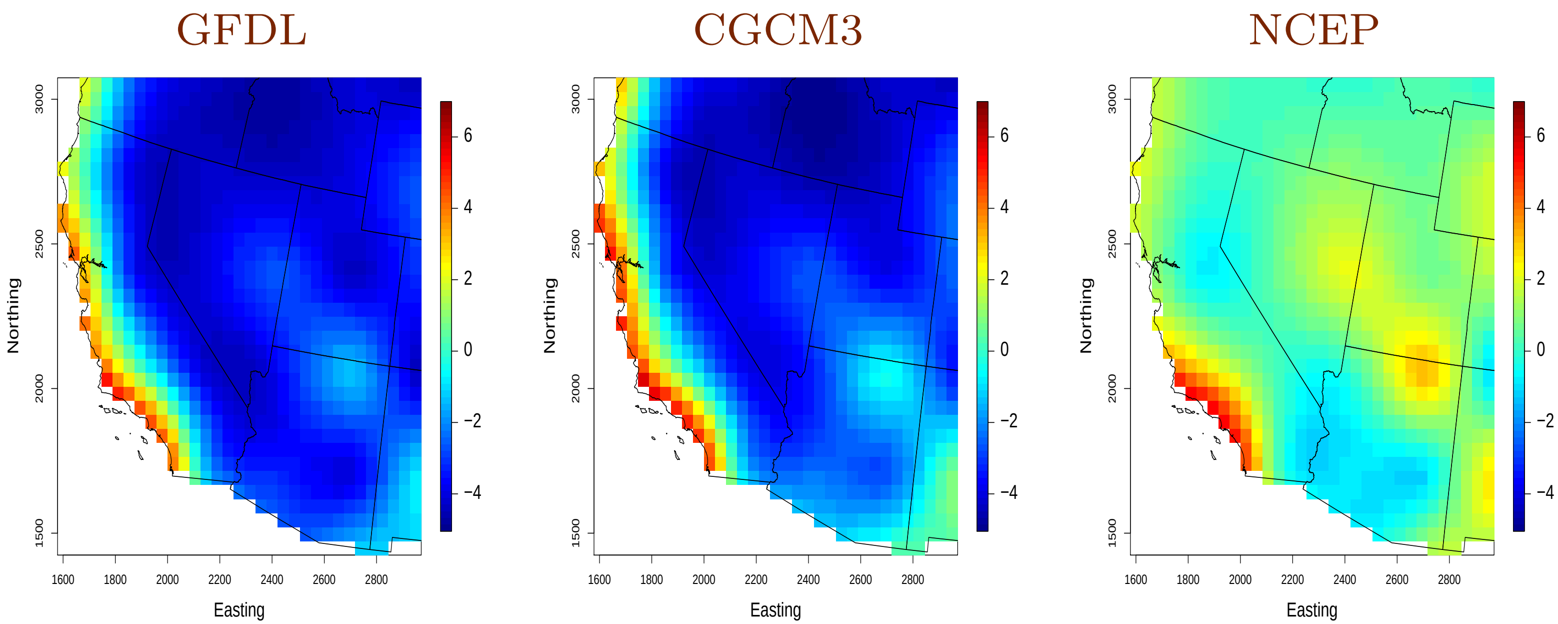
GFDL
CGCM3
NCEP
Northing
Easting
1500
2000
2500
3000
1600
1800
2000
2200
2400
2600
2800
6
4
2
0
−2
−4

Constant Discrepancy Coefficients

α_1

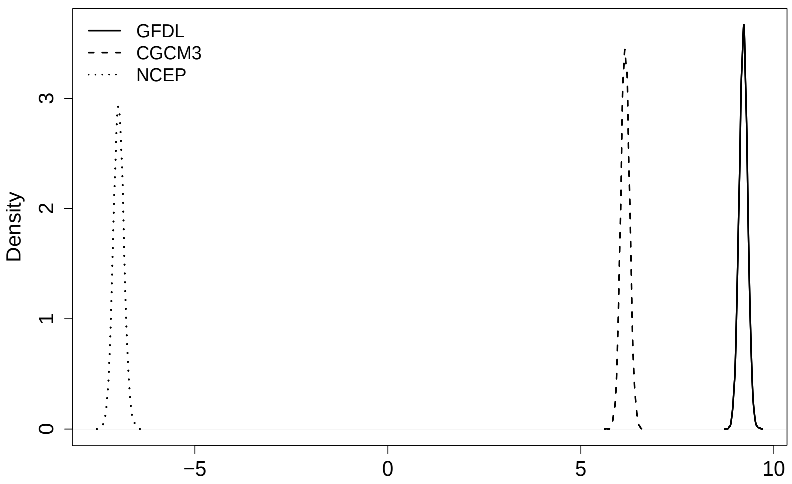

α_2

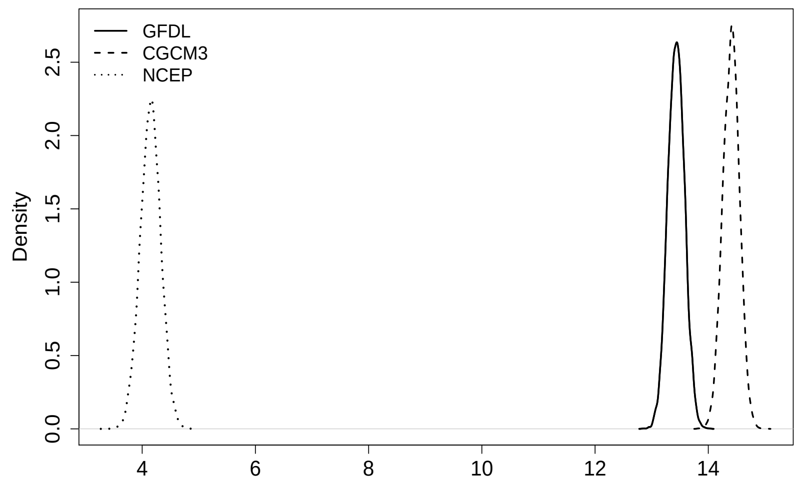

α_3

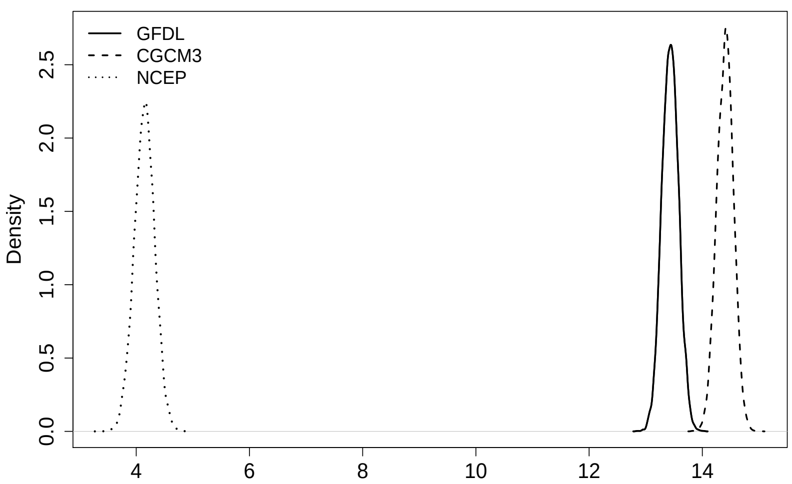

α_4

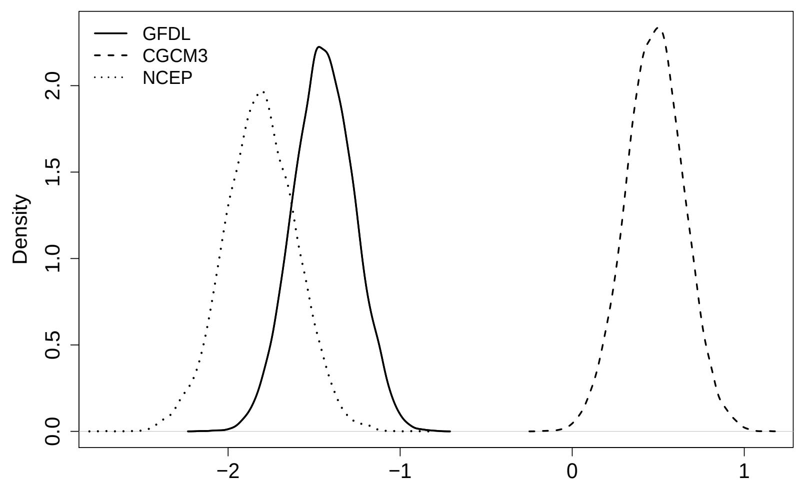

We assess our future predictions by taking a training set (1971–1990) and a test set (1991–2000). We consider:

- Continuous rank probability scores.
- Energy scores
- Root mean square error
- Mean absolute error

Forecast	**CRPS**	**ES**	**RMSE**	**MAE**
CGCM3	2.91	108.80	3.98	3.38
GFDL	3.20	115.50	4.17	3.67
Merged	3.01	110.40	4.06	3.51
Observations	0.59	20.15	1.03	0.79
Model 1 (32 knots)	2.19	74.20	3.53	2.95
Model 2 (32 knots)	**1.20**	**42.94**	**2.14**	**1.69**
Model 2 (68 knots)	1.22	43.72	2.17	1.70

Forecast	**CRPS**	**ES**	**RMSE**	**MAE**
CGCM3	2.91	108.80	3.98	3.38
GFDL	3.20	115.50	4.17	3.67
Merged	3.01	110.40	4.06	3.51
Observations	0.59	20.15	1.03	0.79
Model 1 (32 knots)	2.19	74.20	3.53	2.95
Model 2 (32 knots)	**1.20**	**42.94**	**2.14**	**1.69**
Model 2 (68 knots)	1.22	43.72	2.17	1.70

All three statistical procedures improve the predictions of the model runs. The best method is obtained with a coarse grid and constant discrepancies.

Predicted Time Series

Idaho

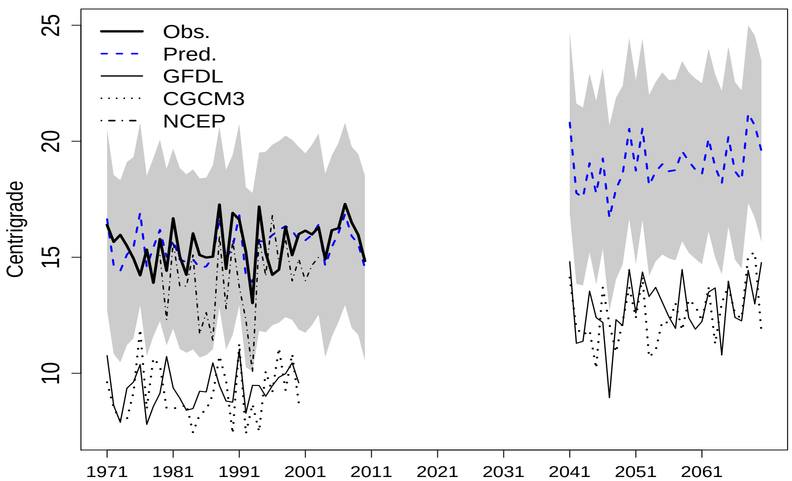

Utah

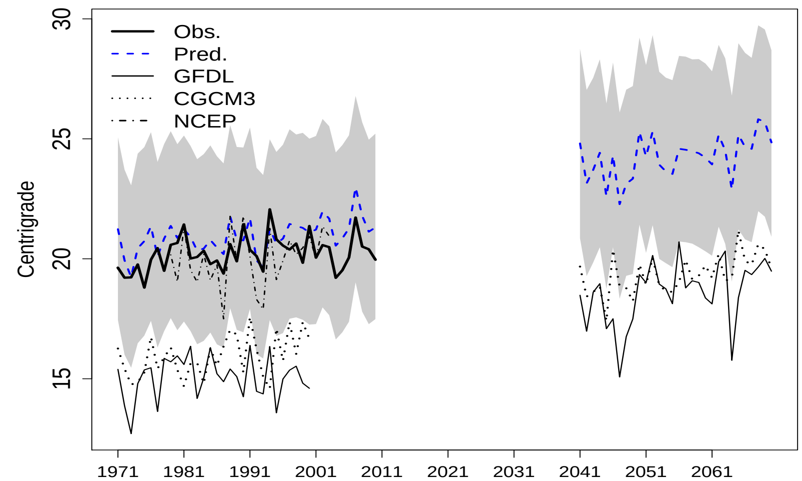

California

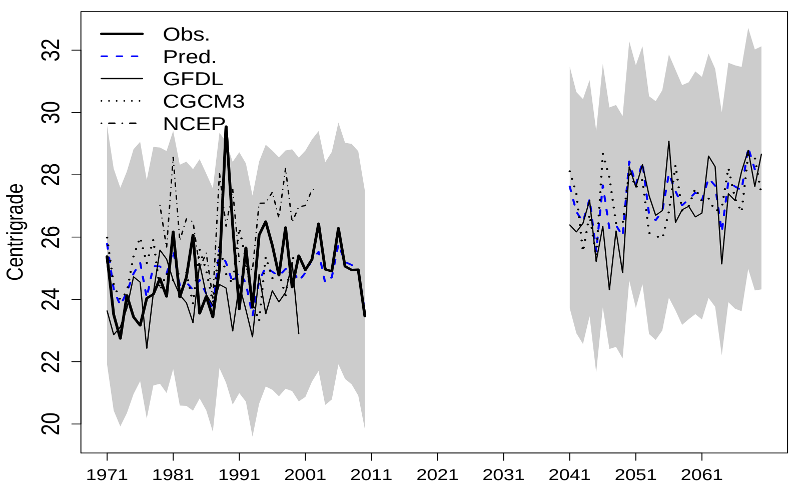

Arizona

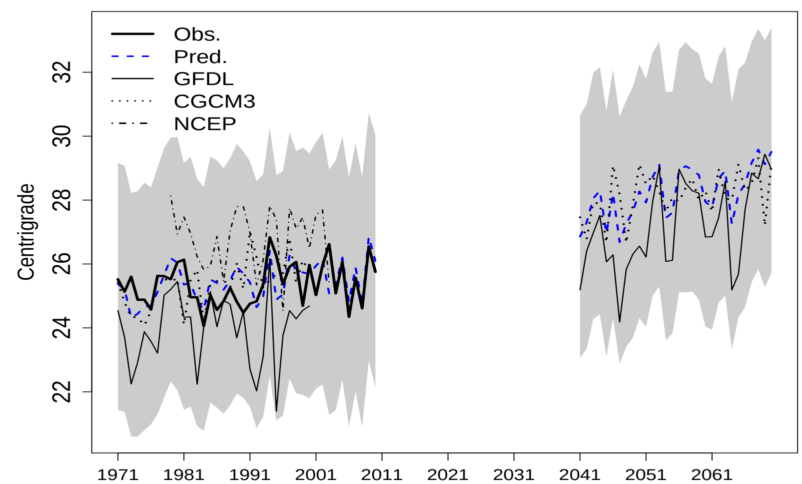

Average Predictions 2041–2070

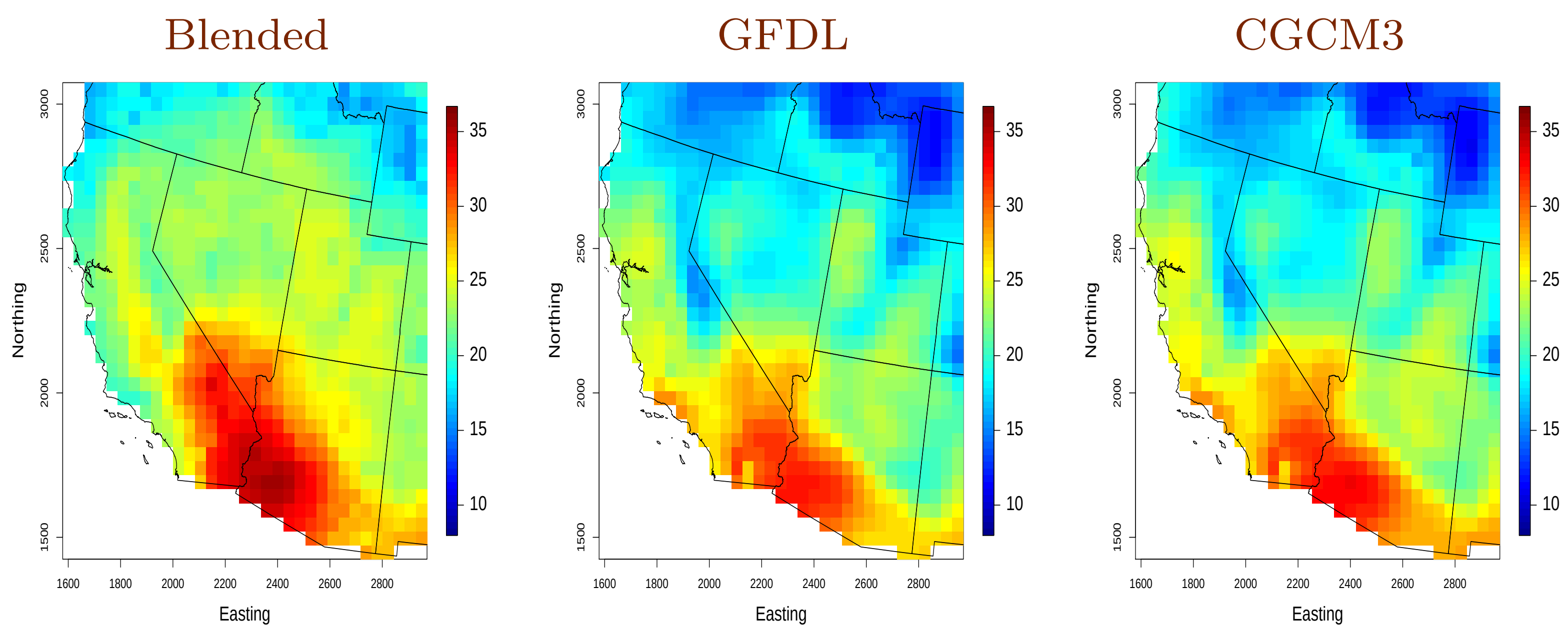

Blended Predictions

2070

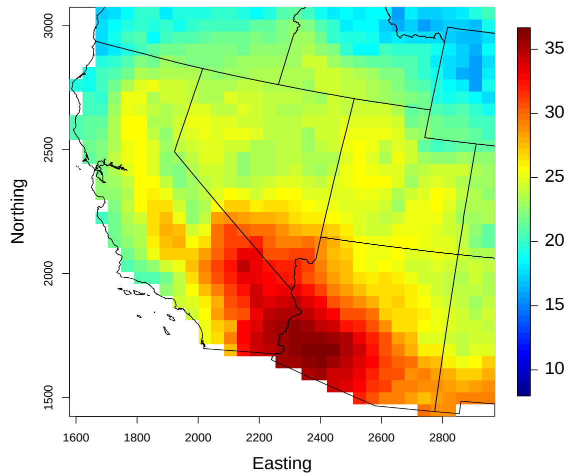

2070 - 2010

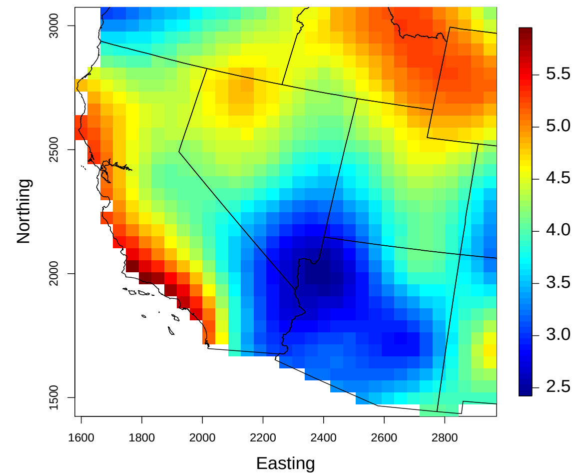

Prob(diff>3°)>85%

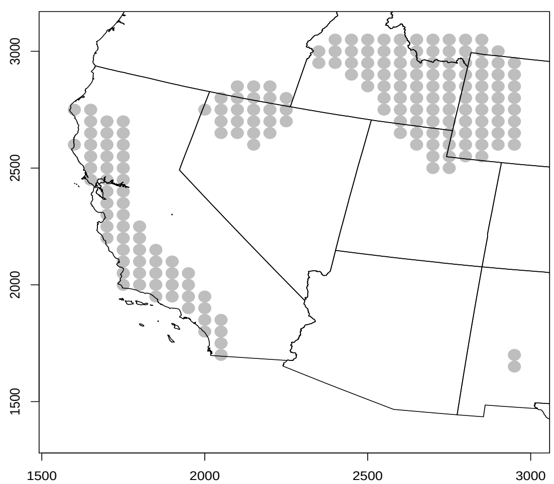

Prob(diff>3°)>90%

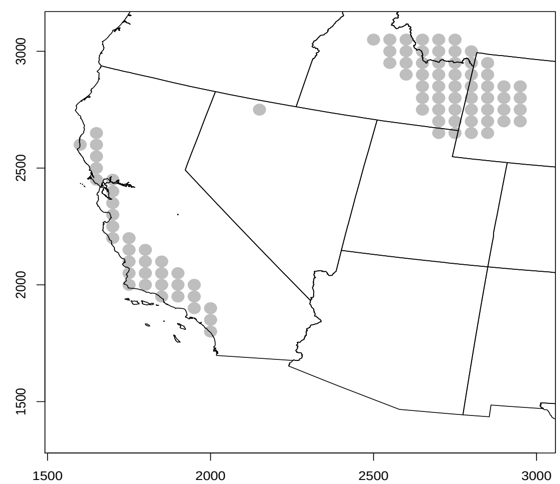

- We use hierarchical models to compare and blend information from different climate model simulations and obtain unified predictions.

- We use hierarchical models to compare and blend information from different climate model simulations and obtain unified predictions.
- Our model provides a quantification of the uncertainties associated with the predictions.

Conclusions

- We use hierarchical models to compare and blend information from different climate model simulations and obtain unified predictions.
- Our model provides a quantification of the uncertainties associated with the predictions.
- We use spatial and temporal models to introduce smoothing in time and space.

- We use hierarchical models to compare and blend information from different climate model simulations and obtain unified predictions.
- Our model provides a quantification of the uncertainties associated with the predictions.
- We use spatial and temporal models to introduce smoothing in time and space.
- Our spatial factor model reduces computations and allows for the description of patterns, cycles and trends that can be used as summaries of the analysis.

- Esther Salazar, Bruno Sansó, Andrew Finley, Dorit Hammerling,Ingelin Steinsland, Xia Wang and Paul Delamater (2011) “Comparing and Blending Regional Climate Model Predictions for the American Southwest”. Journal of Agricultural Biological and Ecological Statistics, 16, 586–605.
- Francisco Beltrán, Bruno Sansó, Ricardo Lemos and Roy Mendelssohn (2011) “Joint Projections of North Pacific Sea Surface Temperature from Different Global Climate Models”. To appear in *Environmetrics*.

References

- Claudia Tebaldi and Bruno Sansó (2009) "Joint Projections of Temperature and Precipitation Change from Multiple Climate Models: A Hierarchical Bayes Approach" *Journal of the Royal Statistical Society Series A*, vol. 172, pp. 83–106.
- Mark A. Snyder, Bruno Sansó and Lisa C. Sloan (2007). "Validation of Climate Model Output using Bayesian Statistical Methods". *Climatic Change*, vol 83, pp 457–476, 10.1007/s10584-007-9262-3.
- Bruno Sansó and Lelys Guenni (2004) "A Bayesian Approach to Compare Observed Rainfall Data to Deterministic Simulations", *Environmetrics*, vol 15, pp. 597–612.